

Safety Analysis of Nuclear Containment Structure against Aircraft Crash and Induced Fire

A. Rawsan¹, M.A. Iqbal² and M.R. Sadique³

¹Civil Engineering Department, Graphic Era University, India

²Civil Engineering Department, Indian Institute of Technology Roorkee, India

³Research Scholar, Civil Engineering Department, Indian Institute of Technology Roorkee, India

E-mail: ¹rawsance@gmail.com, ²iqbalfce@iitr.ac.in, ³rehan.sadique@gmail.com

Abstract—Nuclear energy presently contributes more than 17% of global energy demand. There are 20 working, 7 proposed and 5 under construction Nuclear Power Plants (NPP) in India. In view of the recent nuclear disasters, safety concern in nuclear structures is on the rise. In this study, safety analysis of the outer containment of a typical NPP has been carried out using finite element code ABAQUS 6.10. To maximise the impact effect, the wall is considered as flat in the present study. However, to perform a system efficient simulation, only a quarter of the wall has been modelled.

A 1.2 m thick doubly reinforced concrete wall has been simulated. The behaviour of concrete has been incorporated using Concrete Damaged Plasticity model while that of the reinforcement Johnson Cook elastic-visco plastic model. The material parameters at elevated temperature have been taken from Eurocode 2. Reaction time response curve of Boeing 707-320 has been employed to find the response of containment against aircraft crash. Thermal stress analysis has been performed by combining the impact and heat effect together. It has been assumed that fire starts 0.16 sec. after the application of impact load. A maximum deformation of 48 mm has been noticed. Maximum temperature was found to be 974 °C.

1. INTRODUCTION

The safety assessment of important structures, such as a nuclear power plant, for the crash of a large commercial aircraft has been performed worldwide after the terrorist attack that occurred in the U.S. on September 11, 2001. However, many important studies on this subject were carried out much before these attacks in order to study the effect of accidental crash of various aircraft on important structures (e.g. Riera 1968, 1980; Abbas et al. 1996; Arros and Doumbalski 2007). The nuclear containment is constructed in two layers of reinforced concrete shell. The purpose of the inner containment is to control the emission of radioactive radiation while the outer containment provides safety against possible external threat. For the external containment wall, aircraft crash and its subsequent fire effects on a nuclear containment structure may present the most serious threat to its integrity and stability. However, taking into consideration the massive cost and human efforts required, it becomes extremely difficult to study the behaviour of the containment for both the impact and thermal effect through experiments. Therefore,

many researchers have attempted to numerically simulate the response of containment during an aircraft crash. An analysis of an air-craft crash on an outer containment of a nuclear power plant by taking into account the result of target yielding simultaneously with the reaction time in a time marching scheme was done by Abbas et al. 1995. Studies have also been performed for determining the response with changed cracking strains and different locations of aircraft impact for different aircraft. Kukreja 2005 analysed Indian nuclear containment using load by time history for Boeing 707-320 and other aircrafts. Similarly, Jeon et al. 2012 evaluated the fire resistance of a nuclear power plant subjected to a large commercial aircraft crash. A 3-D FEM model of the containment and auxiliary building was prepared and used for the heat transfer and thermal stress analysis, taking into account the material properties at an elevated temperature. It was found that a considerable magnitude of section forces such as bending moment and axial force were generated by the internal and external restraints imposed by the thermal deformation. The magnitude of these forces was quite large; thereby, these were regarded as the primary forces in safety assessment.

The present study focuses on the studying the behaviour of a nuclear containment of outer concrete layer 1.2 m thick and 30m high against the impact of an aircraft and its subsequent fire induced stresses. As discussed earlier, some work has already been done on this type of problem where the force history curves obtainable by many authors or an actual/ arbitrary model of an aircraft was made to hit over the outer containment wall to see the behaviour of the structure and its failure. It has also been known by many researchers that the concrete material exhibits dissimilar behaviour under different conditions of loading such as compressive or tensile loading, rate of loading, strain rate variation, temperature etc. Aircraft crash on containment is a complicated subject where such varied behaviour is encountered. Thus the plastic behaviour of the concrete has been integrated in the present study using the concrete damaged plasticity model available in Abaqus/Implicit, a finite element solver software. The change

in rate of loading produces variation in the strain rate in the concrete material. This effect has been incorporated using the strain rate dependent data for the concrete. Further, it is obvious that after the impact heat will be generated due to the fuel spillage on to the surface and bottom of the containment. This heat can generate temperatures as high as 1200 degrees Celsius because of which thermal stresses will be induced in the structure along with the impact stresses. Hence, the material properties of concrete at elevated temperature have to be taken in to consideration. These properties are taken from Eurocode 2, 2004.

In the initial stage, the impact force of an aircraft over outer flat plate was applied at mid-level of the plate structure using the Riera 1980 force history curves. Following the aircraft impact, the thermal stress analysis has been performed to understand the behaviour of the containment. For this analysis, fire is assumed to continue for 2 hours at bottom level of the containment up to a height of 10 meters from base (Jeon et al. 2012).

2. NUMERICAL METHODOLOGY

The modeling and meshing of the containment structure was done in Abaqus CAE. The containment structure was made up of RCC suitably reinforced using Fe- 415 steel bars. The containment structure is made up of cylindrical wall but flat plate has been taken to analyse the structure as given in Fig. 1. The flat plate is of uniform thickness throughout the geometry. The outer containment of the nuclear power plant was modeled using Abaqus 6.8 as a three dimensional deformable solid plate of 1.2 m thickness. The containment was suitably reinforced using steel bars modeled as 3D wire (truss) elements. 40 mm diameter rebars were used as both vertical and horizontal reinforcement with an effective cover of 100 mm on all sides. The centre to centre spacing between the bars was 80 mm in both the directions. Modeling of reinforcement in the outer face of the containment structure is shown in Fig. 2. The contact between the reinforcement and concrete was simulated by embedding steel rods in the concrete material. The option is available for such an interaction between reinforcement and 3D solid element in Abaqus FE solver by providing embedded constraint between the two with reinforcement as embedded element and the concrete as the host element. This ensures perfect bond between steel and concrete without any slip between the two materials. Also the base of the containment structure (two sides of plate) is assumed to be rigid and thus was provided with the fixed boundary conditions. The plate was provided with symmetric boundary conditions on the other two sides such that the deformations in the plane normal to the axis of loading was the same as at the principal cutting plane. This method follows the approach used by Kukreja 2005.

It is quite difficult to calculate precisely the force exerted by a striking air craft over the target structure at the point of impact. Further, the behaviour of the material over the impact

region is very difficult to analyse. Therefore, many scientists have tried to propose simplified impact load-time curves for easy application to theoretical analysis. Riera 1980 calculated the reaction force for the deformable aircraft over the target area and plotted the response as the force history curves. These force history curves for Boeing 707 aircraft have been used for applying the loading over the target structure. In the present model, a load of 90 MN was applied over an area of twenty eight square meters in the form of force history curves for Boeing 707-320 Airbus as shown in Fig. 3. The application of load for normal impact of Boeing 707 aircraft on target area is shown in Fig. 1.

A detailed mesh convergence study was done on the basis of heat transfer analysis. A simple plate of 1.2m thick was taken and was meshed with the element size ranging from 600mm to 37.5mm along the thickness of the plate with the aspect ratio of 1. Output Temperature NT11 was noted at various nodes along the thickness of the wall. These values were plotted against the depth of the wall (see Fig. 4). From the graph it can be seen for 32 elements along the thickness of the plate heat penetration depth is the least and it increases with the decrease in number of elements. From this study, 6 elements along the thickness were selected as it allows a sufficiently refined mesh while also exhibiting good agreement with other lower number of elements (2 and 4-elements). This judgment was made keeping in view of time requirement for impact analysis too, as if more number of elements were to be taken along the thickness, the overall number of elements of the containment will increase resulting in higher computational time and effort.

For impact analysis concrete was meshed with 200mm solid elements with reduced integration (C3D8R). Similarly, 2-noded linear 3D truss elements (T3D2) were used to mesh the reinforcement. A mesh size of 600 mm was adopted for the same in the impact region. This was followed by the heat transfer and thermal stress analysis for the RC plate. In these studies, the model was meshed with same element size as previous but the element types were DC1D2 for reinforcement and DC3D8 for concrete model.

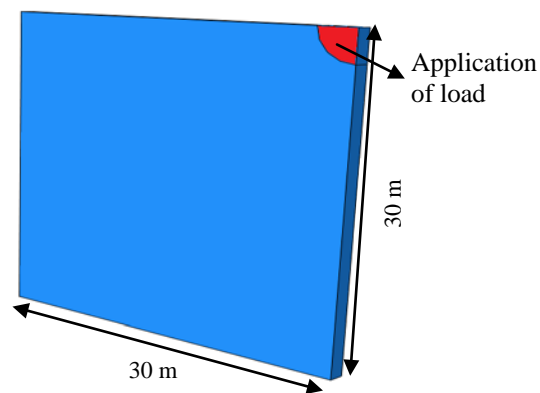


Fig. 1: Outer containment structure.

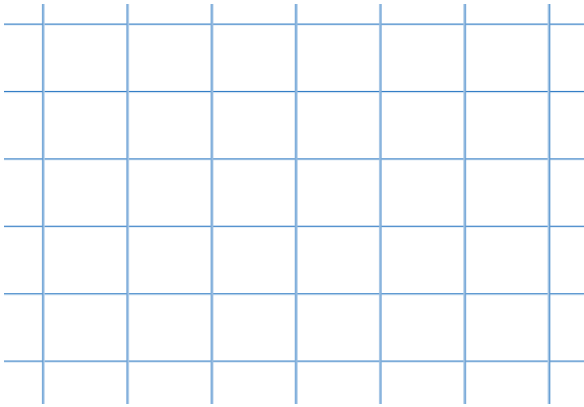


Fig. 2: Reinforcement details at outer face of plate.

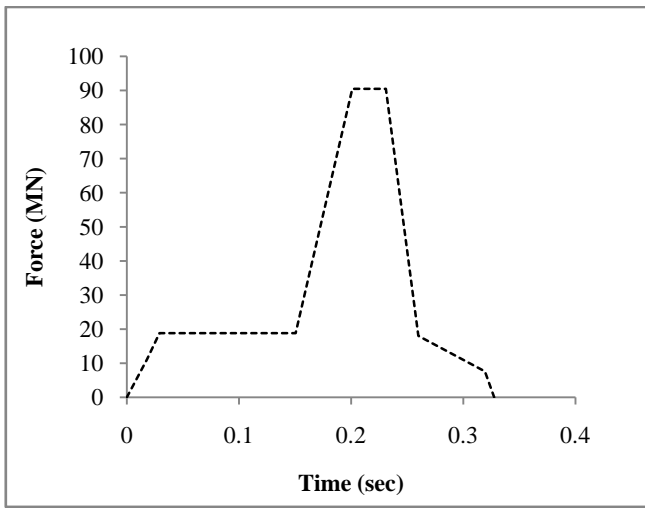


Fig. 3: Reaction time response of Boeing 707-320 Airbus.

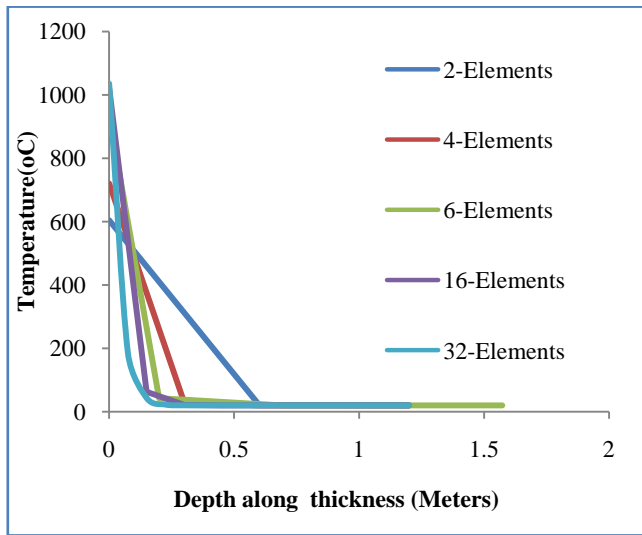


Fig. 4: Variation of temperature along the thickness with different no. of elements.

3. CONSTITUTIVE MATERIAL MODEL AND PROPERTIES OF CONCRETE

Concrete damage plasticity model of Abaqus 6.8 material library was used for the simulating the behaviour of concrete in the containment structure. It is a phenomenological model which can be executed both in Abaqus standard as well as explicit analysis techniques. The material incorporates the plastic behaviour of the concrete both in compression as well as in tension. The model uses the concept of isotropic damaged elasticity in combination with isotropic tensile and compressive plasticity to represent the inelastic behaviour of concrete. It can effectively be used for plain concrete even though it is intended primarily for the analysis of reinforced concrete structures subjected to monotonic, cyclic, and/or dynamic loading under low confining pressures. The model has the provision to use strain rate dependent behaviour of the concrete.

The plasticity based damage model for concrete assumes that the two main failure mechanisms are tensile cracking and compressive crushing of the concrete material. The evolution of the yield (or failure) surfaces is controlled by two hardening variables, $\tilde{\epsilon}_t^{pl}$ and $\tilde{\epsilon}_c^{pl}$ linked to failure mechanism under tension and compression loading, respectively. $\tilde{\epsilon}_t^{pl}$ and $\tilde{\epsilon}_c^{pl}$ referred to tension and compression equivalent plastic strains, respectively. Generally under the uniaxial tension the stress-strain response of the concrete material follows a linear elastic relationship until the value of the failure stress, σ_{t0} is reached. The failure stress corresponds to the onset of micro-cracking in the concrete material. When the concrete specimen is unloaded from any point on the strain softening branch of the stress-strain curves, the unloading response is weakened, the elastic stiffening of the material appears to be damaged. The degradation of the elastic stiffness is characterized by two damage variables, d_t and d_c , which are assumed to be functions of the plastic strains, temperature, and field variables:

$$d_t = d_t(\tilde{\epsilon}_t^{pl}, \theta, f_i) i \quad 0 \leq d_t \leq 1$$

$$d_c = d_c(\tilde{\epsilon}_c^{pl}, \theta, f_i) i \quad 0 \leq d_c \leq 1$$

The damage variables can take values from zero, representing undamaged material, to one, which represents total loss of strength. The stress-strain relationship under uniaxial tension and compression loading are, respectively:

$$\sigma_t = (1 - d_t) E_0 (\epsilon_t - \tilde{\epsilon}_t^{pl}) \quad \sigma_c = (1 - d_c) E_0 (\epsilon_c - \tilde{\epsilon}_c^{pl})$$

Under the uniaxial cyclic loading the model assumes the reduction of the elastic modulus in term of a scalar degradation variable d as

$$E = (1 - d) E_0$$

Fig. 5(a) and 5(b) shows the stress-strain curves for the concrete material under uniaxial loading in tension and compression.

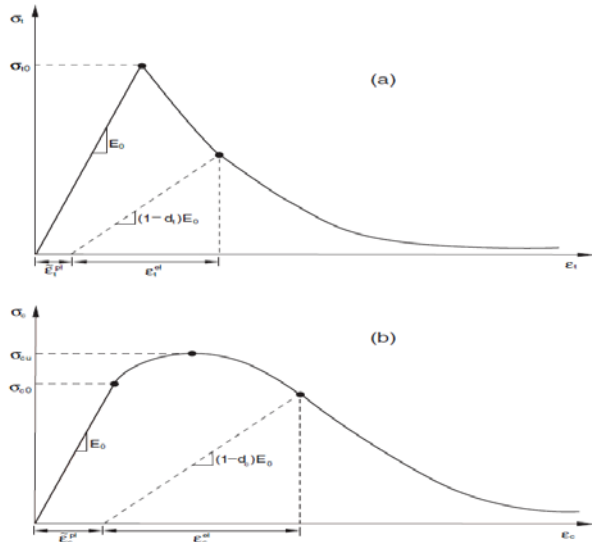


Fig. 5: Response of concrete to uniaxial loading in tension (a) and compression (b).

4. BASIC MATERIAL PROPERTIES OF CONCRETE

Density, ρ (kg/m ³)	2400
Modulus of elasticity, E(N/m ²)	2.7386E+10
Poisson's ratio, ν	0.17
Dilation angle, ψ	30
Eccentricity	1.0
f_{bo} / f_{co}	1.16
K	0.666

Sinha et al. 1964 carried out cyclic loading tests on 25.8 MPa cylinders at very low strain rate (Fig. 6(a)). Grote et al. 2001 carried out experiments at varying strain rates (Fig. 6(b)). The compressive strength of concrete in the numerical simulations carried out by Abbas et al. 1996 was 35 MPa. The tensile strength has been taken from Lu and Xu 2004.

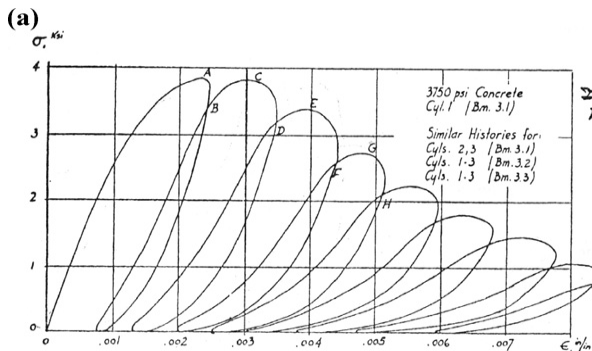


Fig. 6: (a). Concrete behavior under compression: Sinha et al. 1964 for low strain rate.

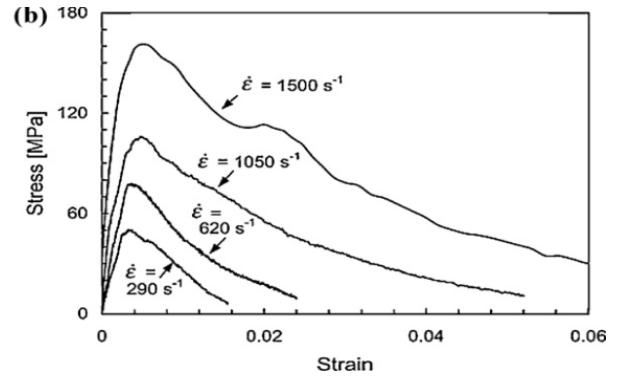


Fig. 6: (b). Concrete behaviour under compression: Grote et al. 2001 for high strain rate.

For the purpose of this study the fracture energy has been taken to be 720 N/m, i.e. 8 times to the fracture energy adopted by Hillerborg, defined in Abaqus manual 6.8. For concrete of 35 MPa the fracture energy at quasi-static loading is taken as 90 N/m.

The stress strain curve for concrete as well as reinforcement at elevated temperature has been taken from Eurocode 2.

Similarly the remaining materials properties have been taken from Eurocode 2, Iqbal et al. 2012 and Sadique et al. 2013.

5. RESULTS AND DISCUSSIONS

In order to understand the behaviour of the nuclear containment structure numerical simulation has been carried out in a FEA tool based on the available literature. Riera force history curve was used as an amplitude load applied on the containment over 28m² area at the mid height of the containment. Concrete behaviour is modeled by using damaged plasticity model. The steel rebars were embedded in concrete for stress analysis. For the heat transfer analysis of the containment, tie constraint was used between steel and concrete. The results of different phases of this study are discussed below.

6. HEAT TRANSFER ANALYSIS

Fire scenario on the external surface of the plate due to aircraft crash was studied by making partitions based on the severity of the heat exposure. It was assumed that the impact region will experience heat for the lesser time as the fuel after the impact gets spilled over the entire surface. On the other hand, as the fuel spreads on the floor of the structure, the possibility of the flames spreading and affecting up to 10 meters height may be considered as severe. Fig. 7 shows the jet fuel curve for fire (Jeon et al. 2012) and at impact region fire curve was modified to a lower duration(700°C for 15 minutes).

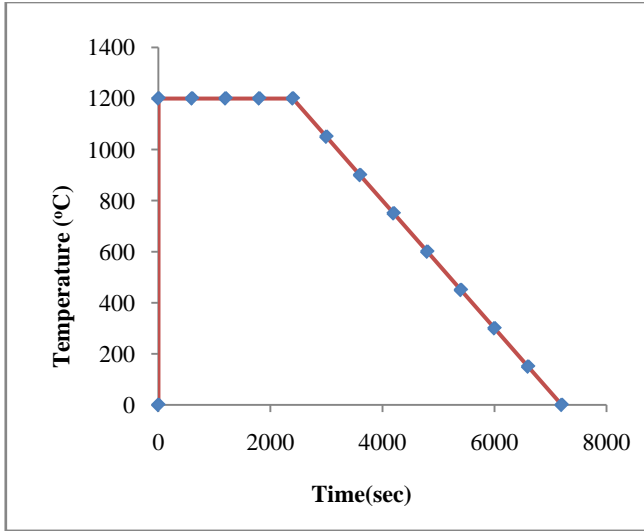


Fig. 7: Proposed jet fuel curve for high exposed surface (bottom).

Ambient temperature was kept as 20⁰C. Variation of temperature along the thickness has been shown in Fig. 8 for 3023 sec. From the Figure, it is clear that at advanced stage of fire exposure, the temperature is highest at the outer nodes and decreases linearly up to a depth of 200 mm to ambient temperature (20⁰C). Further, different nodes at outer surface were examined along the height of the plate both for concrete and reinforcement. These node numbers are Node no. 56169(at impact region),14534(20m from base),42713(5m from base) in concrete and 2214(5m from base), 639(20m from base), and 4232(at impact region) in outer reinforcement. The temperature at these nodes is presented at different time steps in Figures 9(a) and 9(b).

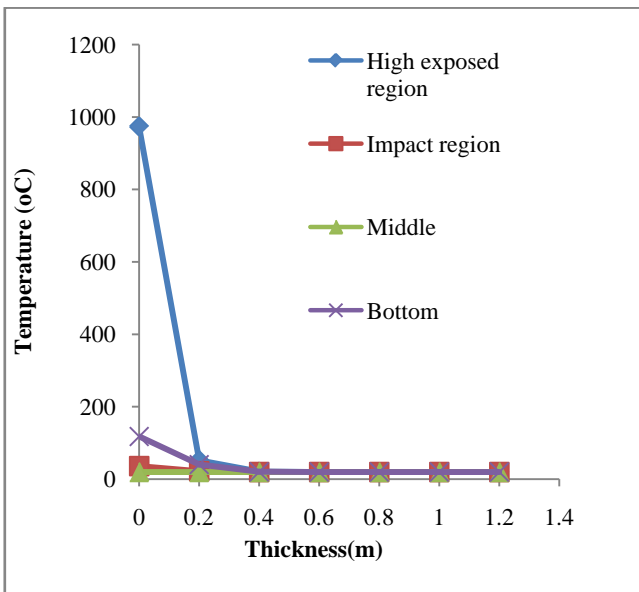


Fig. 8: Temperature variation along thickness.

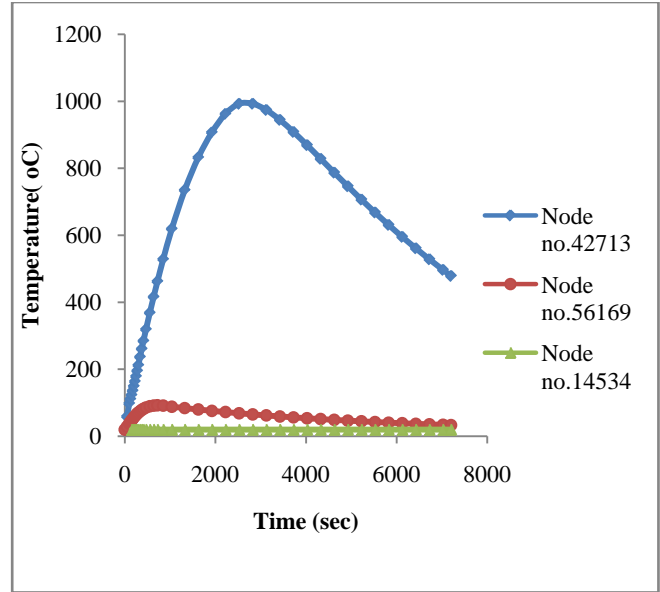


Fig. 9: (a). Variation of Temperature at different outer surface nodes in concrete with varying time.

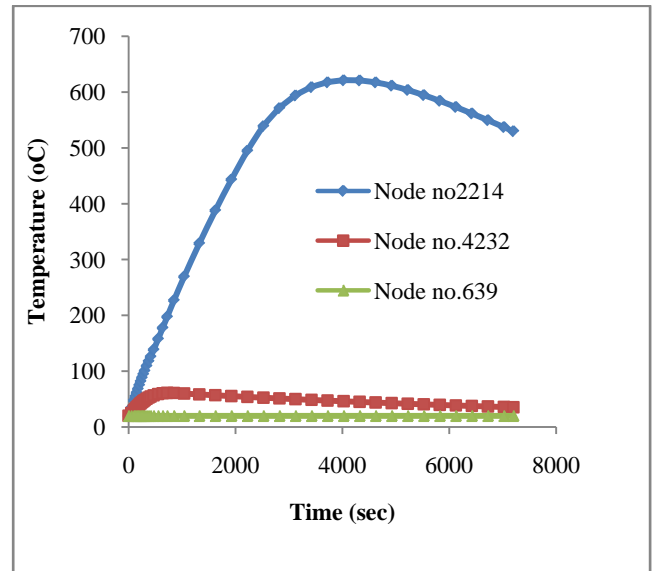


Fig. 9: (b). Variation of Temperature in reinforcement with time at various outer surface nodes.

7. IMPACT ANALYSIS

In a sequence, impact analysis was performed on the same model with same mesh configuration, thereby retaining the nodal numbers of the model used for the heat transfer analysis. Strain rate dependent data was used for the material properties. The plate was assumed to be subjected to impact load for a time period of 0.16 sec. The load was applied using Riera 1980 amplitude time history (see Fig. 3). The deformed shape of the containment is shown in Figures. 17. The

maximum deformation was observed to be 47.67 mm in impact region (Fig. 10). Fig. 11 and 12 shows the stress along the thickness of plate at impact region and 5m height of the plate.

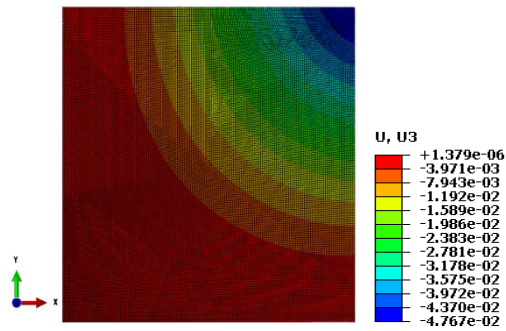


Fig. 10: Deformation profile at time 0.16 sec.

7.3. Thermal Stress Analysis

As mentioned earlier thermal stress analysis is the second step which follows after impact and heat transfer analysis. The deformations and the stresses obtained from the last frame of the step-1 analysis were imported by predefining the initial state of the model in the thermal stress analysis. The thermal stresses were obtained for some selected frames of the heat transfer analysis results. Following graphs show the variation of stresses along the thickness of the wall at the impact region. These have been shown in Figures 13 to 15.

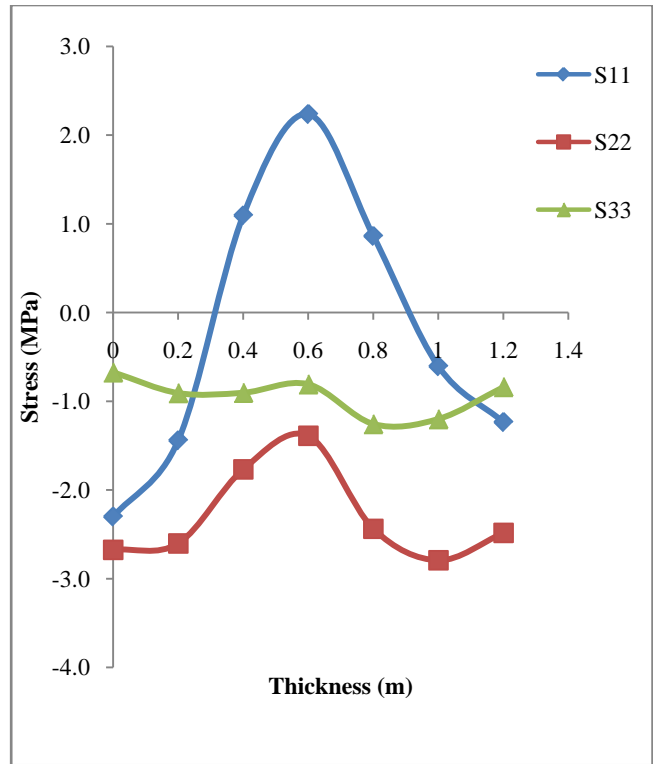


Fig. 12: Variation of stresses along the thickness of the wall at 5m height of plate at time T=0.16 Sec.

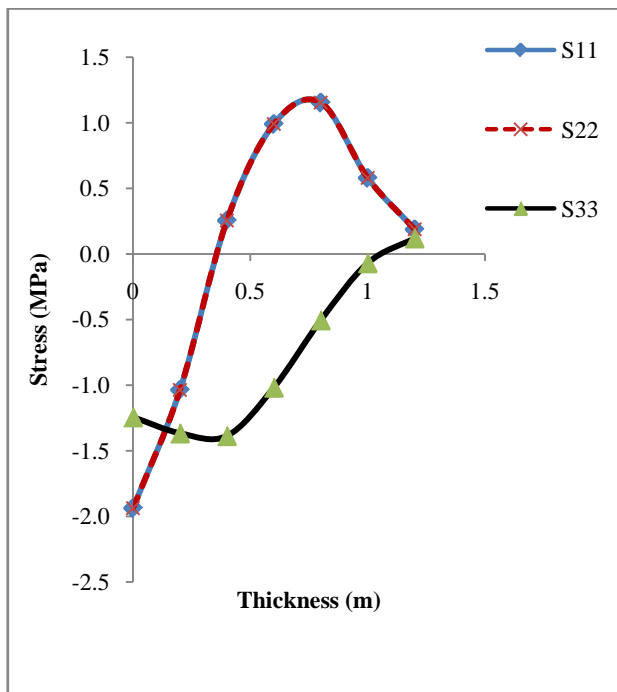


Fig. 11: Variation of stresses along the thickness of the wall at impact region at time T=0.16 Sec.

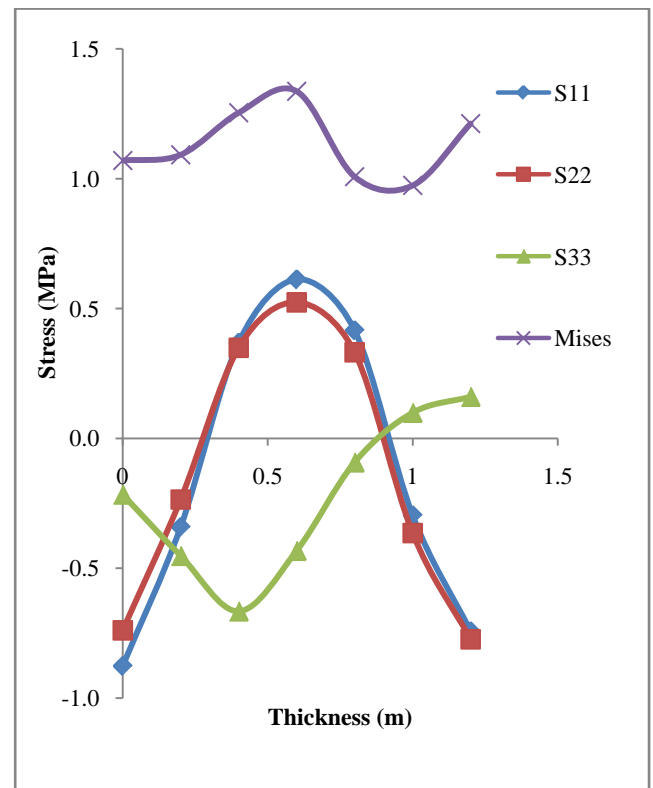


Fig. 13: Stresses variation along the thickness of the plate at time T=100.16 Sec.

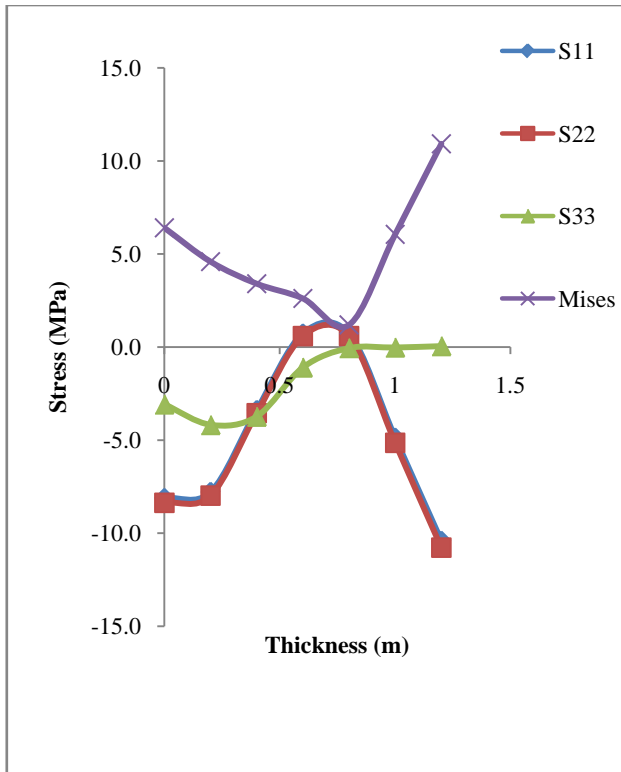


Fig. 14: Stress variation along the thickness of the plate at time T=7200.16 Sec.

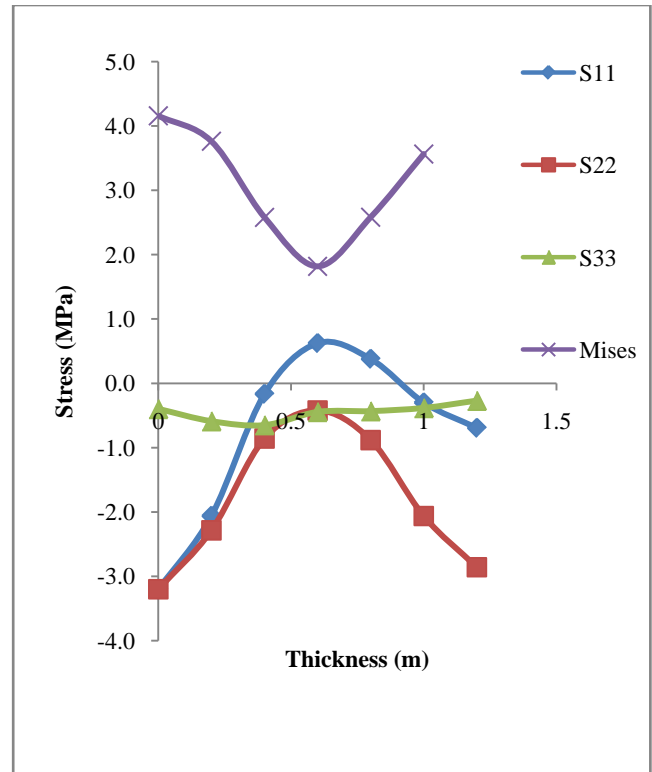


Fig. 16: Stresses variation along the thickness of the plate at time T=100.16 Sec.

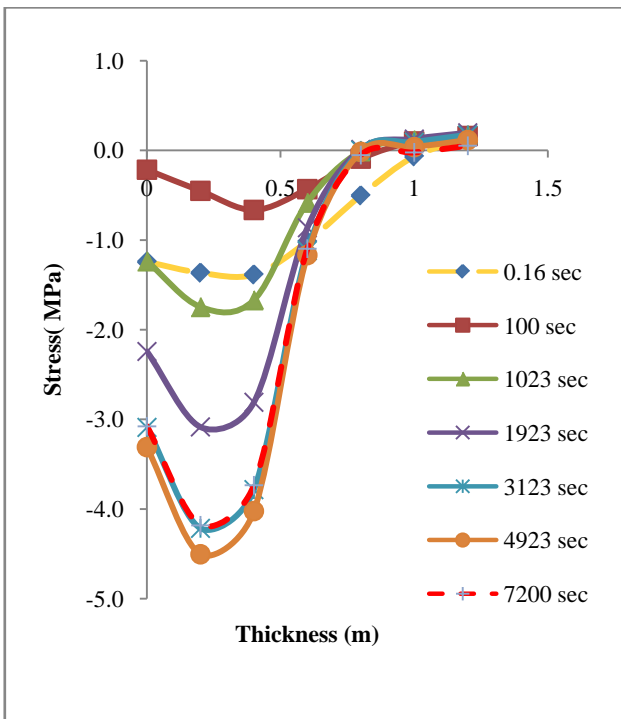


Fig. 15: Normal stress along the direction of loading at different time increment.

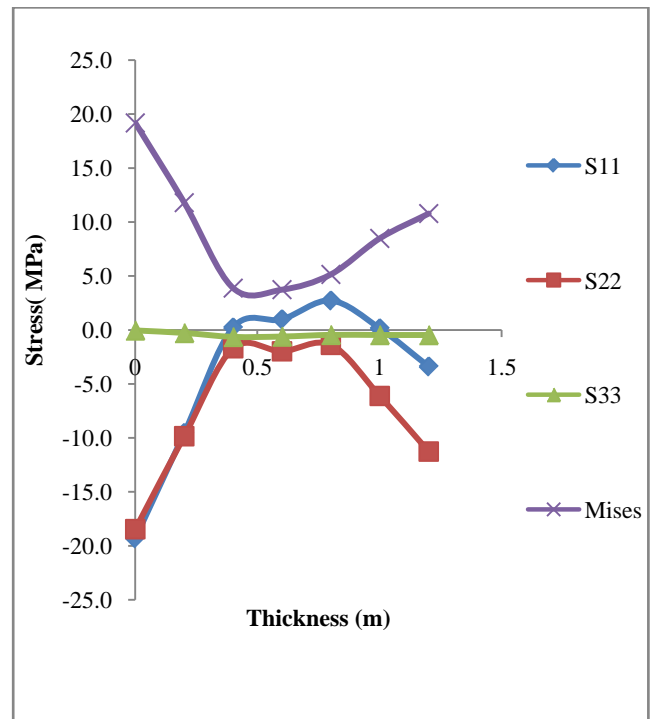


Fig. 17: Stresses variation along the thickness of the plate at time T=7200.16 Sec.

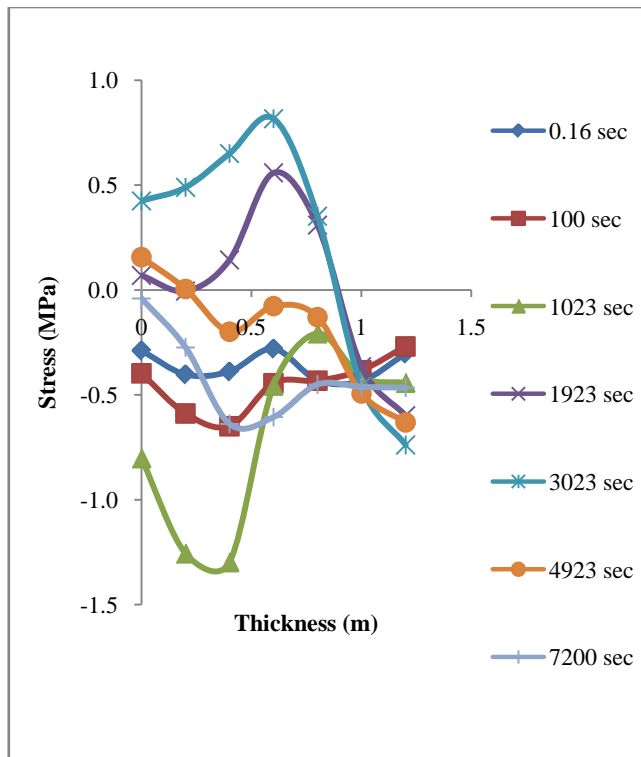


Fig. 18: Normal stress along the direction of loading at different time increment.

From Fig. 15, it can be observed that the outer face of the plate remains in compression throughout the thermal stress analysis. Further, it is seen that stress along thickness varies from nearly 3 MPa compressive at outer face (at the end of fire) to tensile value of 0.2 MPa at inner face of the plate. Similarly, the Figures 16 to 18 show the variation of stresses along the thickness of the wall at highly fire exposed area (5 metres from the bottom face). In contrast to the purely compressive stress values at outer face impact region, the pressure values at 5 m height are found to oscillate between compressive at the beginning of the analysis to tensile near the middle of the post-impact fire. This phase coincides approximately with the peak of the jet fuel curve (see Fig. 3). As the thermal load reduces linearly from maximum to zero, concrete begins to re-exhibit compressive stresses at later stages of the analysis.

8. CONCLUSION

In this investigation an attempt has been made to find out the behavior of the RC plate for an aircraft crash and its subsequent fire effects using finite element code. This was done in two steps. In the first step impact analysis was done on the model followed by a heat transfer analysis. This was followed by thermal stress analysis performed by importing the deformed state of the model as initial condition in the second step. Curves were plotted for the resultant stresses due to impact and fire along the thickness of the wall. The following conclusions were drawn from the study:

1. From the heat transfer analysis it is clear that the maximum penetration of heat along the thickness of containment wall is 200mm and rest of the depth remained at ambient temperature of 20°C. The same was also noticed through the mesh convergence studies carried out.
2. Impact analysis showed a displacement of 47.67 mm (in the direction of impact) for an applied load for 0.16 sec. The stresses induced were nominal for such a small duration of load.
3. Thermal stress analysis showed that the outer face of the plate at the impact region is under compression all through the analysis. On the other hand, highly exposed fire area of concrete was found to be in a varying state of stress, exhibiting compression near the beginning and end of the thermal load accompanied by tensile stresses near the mid-stage of analysis.
4. Thermal stresses produced due to crash induce fire may cause scabbing of concrete leading to exposure of reinforcement. However, the induced fire does not pose a threat to the global behaviour of the containment structure.

REFERENCES

- [1] Riera, J.D. (1968) "On the stress analysis of structures subjected to aircraft impact forces", *Nucl. Eng. Des.* 8, 415-26.
- [2] Riera, J.D. (1980) "A critical reappraisal of nuclear power plant safety against accidental aircraft impact", *Nucl. Eng. Des.* 57, 193-206.
- [3] Abbas, H., et al. "Reaction time response of aircraft crash", *Comput. Struct.* 55 (5), 809–817. 1995.
- [4] Abbas, H., Paul, D.K., Godbole, P.N., Nayak, G.C. (1996) "Aircraft crash upon outer containment of nuclear power plant", *Nucl. Eng. Des.* 160, 13-50.
- [5] Iqbal, M.A., Rai, S., Sadique, M.R., Bhargava, P. (2012) "Numerical simulation of aircraft crash on nuclear containment structure", *Nucl. Eng. Des.* 243, 321-335.
- [6] Sadique, M.R., Iqbal, M.A., Bhargava, P. (2013) "Nuclear containment structure subjected to commercial and Figurehter aircraft crash", *Nucl. Eng. Des.* 260,30-46.
- [7] Jeon, S., Jin, B., Kim, Y. (2012) "Assessment of the Fire Resistance of a Nuclear Power Plant Subjected to a Large Commercial Aircraft Crash", *Nucl. Eng. Des.* 247,11-22.
- [8] Kukreja, M. (2005) "Damage evaluation of 500 MWe Indian Pressurized Heavy Water Reactor nuclear containment for aircraft impact", *Nucl. Eng. Des.* 235, 1807–17.
- [9] Arros, J., Doumbalski, N. (2007) "Analysis of aircraft impact to concrete structures", *Nucl. Eng. Des.* 237, 1241–49.
- [10] Abaqus Explicit user manuals Version 6.8.
- [11] Eurocode 2 (2004) "Design of concrete structures: Part 1-2: general rules-structural fire design", *European Committee for Standardisation, Brussels, BS EN 1992-1-2, 2004.*
- [12] Sinha, B. P., Kurt, H., Tulin, L. G. (1964) "Stress-Strain Relations for concrete Under Cyclic loading", *J. Am. Concrete Inst.* 2 (61), 195–210.
- [13] Grote, D. L., Park, S. W., Zhou, M. (2001) "Dynamic behaviour of concrete at high strain rates and pressures", *International Journal of Impact engineering* 25, 869-886.
- [14] Lu, Y., Xu, K. (2004) "Modeling of dynamic behavior of concrete material under blast loading", *International Journal of Solid and Structures* 41, 131-143.